

Performance of Aluminide and Cr-modified Aluminide Pack Cementation Coated Stainless Steel 304 in Supercritical Water (SCW) at 700°C

Nick Tepylo, Xiao Huang and Shengli Jiang

Carleton University, Ottawa, ON, Canada

Sami Penttilä

VTT Technical Research Centre of Finland Ltd., Finland

Abstract

The choice of materials is of great concern in the construction of Gen IV supercritical water reactors (SCWR), particularly the fuel cladding, due to the harsh environment of elevated temperatures and pressures. A material's performance under simulated conditions must be evaluated to support proper material selection by designers. In this study, aluminide and Cr-modified aluminide coated 304, as well as bare stainless steel 304 as a reference material, were tested in supercritical water (SCW) at 700°C and 25 MPa for 1000 h. The results showed that all three samples experienced weight loss. However, the aluminide coated 304 had 20 to 40 times less weight loss compared to Cr-modified aluminide coated and bare stainless steel 304 specimens, respectively. Based on Scanning Electron Microscope / Energy Dispersive X-ray Spectroscopy (SEM/EDS) and X-ray Diffraction (XRD) analysis results, spinel and hematite Fe_2O_3 formed on bare 304 after 1000 h in SCW while alumina was observed on both coated specimens, i.e. aluminide and Cr-modified aluminide surfaces. Oxide spallation was observed on the bare 304 and Cr-modified aluminide surface, contributing to a larger weight loss. Based on the results from this study, pure aluminide coating with Al content of 10 - 11 wt.% demonstrated superior performance than bare 304 and Cr-modified aluminide coated 304.

Key words: Oxidation, Alloy 304, Pack cementation coating, aluminide, Cr-modified aluminide, supercritical water reactor (SCWR), surface oxide, SEM, XRD

Nomenclature

Acronyms and abbreviations

CVD Chemical Vapor Deposition
EDS Energy Dispersive Spectrometry
F-M Ferritic-martensitic
SCC Stress Corrosion Cracking
SCW Supercritical Water
SCWR Supercritical Water-cooled Reactor
SEM Scanning Electron Microscopy
XRD X-ray Powder Diffraction

1.0 Introduction

The rapid growth in world population and increased living standard has triggered exploration of long term energy solutions such as those provided by nuclear energy [1]. The Generation IV International Forum was formed to jointly develop advanced reactor designs based upon Generation II and III nuclear reactor technologies [2]. To enhance these current nuclear reactor technologies, improvements in four main categories are considered: sustainability, safety and reliability, economics, proliferation resistance and physical protection [2]. There are six technologies currently being developed, one of which is supercritical water-cooled reactors (SCWR). The increased thermodynamic efficiency of Gen IV SCWRs is attributed to the single-phase supercritical water (SCW) as the coolant [3]. While efficiency can be increased to 45%, from 33% of the currently used light water-cooled reactors, the preliminary design of the Canadian SCWR calls for an operating pressure of 25 MPa, and a core inlet and outlet temperature of 350°C and 625°C, respectively [4]. This design specification requires materials for core components that

can withstand a peak temperature much higher than the fluid temperature, and at the same time sustain radiation impact.

Ni-based alloys have been considered as a candidate material because of their ability to maintain their mechanical properties at increased temperatures. Their high strength, toughness and creep resistance at elevated temperatures coupled with their superior oxidation and corrosion resistance in SCW make them a potential candidate [5, 6]. However, the high neutron absorption cross sections and increased vulnerability to radiation damage as compared to iron-based alloys make them an undesirable material for the reactor core [7, 8]. Conversely, ferritic-martensitic (F-M) steels have been considered as a better candidate material because of their low neutron absorption rates, resistance to radiation and swelling upon radiation exposure in addition to their low cost [9, 10, 11]. Their disadvantage is the degradation of mechanical strength at temperatures greater than 650°C [5] and the high levels of corrosion under SCWR conditions [7, 12, 13]. Fe-based alloys containing increased amounts of Ni, particularly austenitic stainless steels, are of interest because of their improved corrosion resistance over F-M steels and their resistance against creep and radiation [14]. Austenitic stainless steels have been shown to maintain their oxidation resistance and mechanical properties up to a temperature of 1000°C in an oxidizing environment [14], making them a suitable choice for the in-core components. However, there are concerns relating to spallation after exposure to harsh conditions [15, 16].

One possible solution to meet the requirements for structural integrity and corrosion resistance is to apply corrosion resistant coatings to these components [17]. Alumina-based oxide scales are known to mitigate many types of corrosion found in SCW conditions such as stress corrosion cracking (SCC), pitting and general corrosion [18]. It has been reported that the addition of Al to stainless steels can increase the high temperature oxidation resistance [19]. To enhance the

corrosion and oxidation resistance of the cast stainless steel CF8C-plus, a diffusion aluminide coating was applied. Testing in 10% H₂O at 800°C showed that the Al-rich coating was effective in providing oxidation and corrosion resistance to the substrate via the formation of an alumina scale [20]. Chemical vapor deposition (CVD) iron-aluminide (Fe-13, 15 and 20 at.% Al) coated T91 and 304L specimens also exhibited excellent performance in water vapor at 700°C as compared to uncoated specimens [21]. Iron aluminide coatings, applied by a slurry process, (a different process from CVD or pack cementation), on ferritic stainless steel steam turbine components also demonstrated improved steam-oxidation resistance at 650°C [22]. However, depletion of Al from the coating due to Al diffusion into the substrate commonly occurs on exposure to temperatures near or greater than 650°C.

In comparison to another commonly employed oxidation and corrosion resistant MCrAlY overlay coatings, diffusional coatings are often thinner (30 to 50 µm) than MCrAlY overlays. The vapour based process also has the capability of coating non-line-of-sight locations and is a batch process in which a large number of parts can be coated at the same time. The current work aims to assess alloy 304 (as baseline reference) and two different pack cementation coatings (aluminide and Cr-modified aluminide) for potential applications in SCWR, by exposing them to SCW at 700°C and 25 MPa for 1000 h. The selection of this elevated temperature was based on the fact that cladding material would be subjected to temperatures greater than that of the coolant (625°C), as proposed in the current Canadian SCWR design.

2.0 Materials and Experimental Methods

The substrate material used in this study was 304 stainless steel with its nominal composition shown in Table 1. Samples were sheared into 20 mm × 20 mm pieces and polished to 600 grit

finish prior to coating. The pack cementation process was carried out in a tube furnace (Model STT-1600C-4-12 by Sentro Tech Corporation, USA) using the pack cementation technique.

The pack powder mixture for aluminide process contained 10% Al (Metco 54NS, -200+325 mesh) + 20% Ni (Metco 56NS, -200+325 mesh) as the source of the coating, and for chromizing it contained 60% Cr (Alfa Aesar, -325 mesh). The remainder of the powder mixtures consisted of NH_4Cl as the activator, and alumina as the inert filler. The inclusion of Ni in the aluminide coating was twofold; Ni addition has shown to encourage NiAl_2O_4 formation during oxidation, which in turn reduces oxidation rate [22]. The inclusion of Ni in the pack mixture was also to alleviate coating cracking during the process. A 76.2 mm (3") diameter ceramic bowl was used to contain the samples and powders during the coating process. To prepare the pack powder, different powders were weighed using a precision scale (to ± 1 g). Next the powders were put into the bowl and mixed using a mechanical mixer. In order to keep partial pressure and to avoid the escape of the metal halide vapour, a ceramic lid was placed on top of the bowl before being inserted into a tube furnace. Before the temperature was raised to the set point, Ar purging was initiated for 30 min before the temperature was raised. Ar flew continuously during the pack process. The process temperatures were 1000°C for aluminizing (no Cr in the pack) and 1100°C for chromizing, a similar temperature range as that reported in [23]. A duration of 240 min was used for both processes. The Cr-modified aluminide coating composition was achieved using a two-step process, chromizing followed by aluminizing. Prior to coating the test samples for this study, trial runs were carried out using different temperatures and durations. The final process parameter selections were based on the coating structures shown in Figure 1 (a and b) where both coating layers reached about 50 μm to allow for subsequently surface grinding to 600 grit finish. Note that on the surface

there existed loose particles from the pack and micro-cracks on aluminide coatings. Subsequently polishing removed surface imperfections prior to SCW testing.

The coated samples were ground in the following order by using 240, 320, 400 and 600 grit SiC abrasive papers, a standard practice developed for SCW and steam oxidation test at the authors' lab. Approximately 25 μm surface layer has been removed from each sample. After grinding, the samples were cleaned in an ultrasonic bath (Branson 2510) using degreasing agent and water sequentially for 15 min followed by 15 min in acetone. EDS analysis was carried out on the ground samples to measure their final surface compositions, as reported in Table 2. Finally, sample dimensions (using a Mitutoyo micrometer) and weights (with a Mettler Toledo AG285 balance) were measured (Table 3). After SCW testing, samples were weighed again to obtain mass change per unit surface area.

The corrosion exposure test was carried out in a custom built SCW autoclave at 700°C/25 MPa with 150 ppb dissolved oxygen in the inlet flow and a pH of 7 (measured at room temperature in the low pressure part of the recirculation loop). The test durations were up to 1000 h. The autoclave is connected to a recirculation water loop, Figure 2. The high pressure loop consisted of a high pressure pump, heat exchanger, preheater and cooler. The flow rate during the exposure was around 7 mL/min (of water) resulting in refresh time of the autoclave roughly every two h. Specimens were hung on the specimen holder rack using electrically insulating ZrO_2 rings.

Following 1000 h of testing, the surface microstructures were characterised using Scanning Electron Microscope / Energy Dispersive X-ray Spectroscopy (SEM/EDS). Samples were also evaluated along the cross-section. Phase composition of the surface oxides were analysed after

using X-ray Diffraction (XRD). All tests were carried out within a 2θ range of 10° - 90° (θ is the angle between the incident X-ray beam and the horizontal surface of the sample).

3.0 Results

3.1 Weight change

The weight changes of the bare 304 and coated 304 are shown in Figure 3. The weight change was computed using the weight difference between initial and SCW tested sample divided by the total external surface area of each sample. Also included in the same figure are weight changes of two other materials (800H and 3033) tested under the same condition. Weight loss is usually considered an undesirable attribute of the materials for the SCWR as it decreases the cross section of the structure material and also contributes to material transport (either as spalled particles or dissolved ions) to other parts of the system. From the results obtained in the current study, all specimens exhibited weight loss including bare 304, as well as the aluminide and Cr-modified aluminide coated 304, although the aluminide coated 304 sample had a very minimal amount of weight loss (0.15 mg/cm^2 or $1.5 \times 10^{-4} \text{ mg/cm}^2 \text{ h}$). The mass change in a bare 304 tested under 100% steam (not pressurized) at 700°C was measured to be about $+0.21 \text{ mg/cm}^2$ after 1000 h [24]. The application of an aluminide coating (about 60 at.%) in that study reduced the weight gain to about 0.15 mg/cm^2 . Due to the higher pressure of SCW used in this study more oxidization took place, as shown in our previous study [25]. And the spallation tendency of oxide scale upon cooling has been observed to increase with scale thickness, due to increased stresses and reduced adhesion [26]. Examining Table 3 and Figure 3, it becomes clear that Cr-modified aluminide coating has inferior performance than pure aluminide. The elevated Al in Cr-modified aluminide increases the brittleness of the coating while the higher Cr content may have contributed to the

instability/volatility of chromia scale in high temperature SCW [27]. Indeed, Cr_2O_3 has been reported to react with steam and form volatile species such as $\text{Cr}_2\text{O}(\text{OH})_2$ and $\text{CrO}_2(\text{OH})$ [28].

800H is an alloy that has been assessed for potential fuel cladding in Canadian SCWR [29]. From the results shown in Figure 3, it also suffers weight loss after 1000 h in SCW at 700°C . Among the materials shown in the same figure, alloy 3033 (or alloy 33 with a composition of Fe-31.5Ni-33Cr) demonstrates better performance, i.e., slight weight gain due to oxide formation. Alloy 3033, although with elevated amount of Cr similar to that in Cr-modified aluminide, did not show weight loss. Perhaps the formation of an outer layer of Fe-containing spinel FeCr_2O_4 provided protection to the inner layer of Cr_2O_3 [30] [31]. Detailed analysis of Alloy 3033 and 800H tested in SCW at 700°C was reported previously in [31].

3.2 SEM and XRD Analysis

3.2.1 304

SEM images (Figure 4) of the bare 304 surface after SCW exposure reveal that the corrosion/oxidation has taken place non-uniformly, leaving a surface with porous phase (A1), islands with bright particles (B1) and a flat matrix with remaining grinding marks (C1). EDS analysis of all three areas showed strong oxygen signal, suggesting all three areas have been oxidized. Based on the qualitative atomic percentages of elements measured from A1, it is likely to be hematite (Fe_2O_3 , 60 at.% of O). In area B1, the increased Cr content indicates a possible formation of mixed oxide. Area C1, with a composition between that of A1 and B1, may be a region with mixed oxide as well. A cross section of the tested sample is shown in Figure 5. The oxidation can be observed to have progressed to a depth of $>25\ \mu\text{m}$. The top layer of the oxide (D1) has been spalled off from the sample. EDS analysis results from the spalled oxide (D1) and the remaining layer (E1) suggest spinel compositions. The cross section further illustrates the

nature of intergranular oxidation progression, with oxide outlining partially oxidized grains. From the perspective of both oxide spallation and oxidation depth, alloy 304 shall not be used under the high temperature SCW. Finally, XRD analysis was carried out to identify the phases (Figure 6). Both spinel and hematite are present in the oxide layer, confirming the SEM results.

3.2.2 Aluminide coated 304

The aluminide coated 304 sample surface does not reveal any signs of corrosion pits, cracks or spallation after 1000 h in SCW (Figure 7). Rather, it is covered with small grains of Al containing oxides and the grinding marks are still visible after 1000 h exposure in SCW. EDS analysis of the light particles A2 suggests the nature of these particles being Al_2O_3 (Cr and Fe are likely detected from the underlying coating substrate itself). EDS measurement from the surface of area (B2) confirms the enrichment of Al on the surface, comparing to other elements (Cr and Fe). However, the Ni content on the surface (7% prior to SCW exposure) becomes negligible after SCW exposure, due to increased Al and oxygen content in the oxide layer, and also a possible NiO spallation (hence weight loss) at an earlier stage of the exposure.

The cross section of the sample was also evaluated, with its image and compositions shown in Figure 8. There is a very thin, dense, and intact oxide layer (C2) on the surface. The formation of such protective Al_2O_3 layer resulted in the least amount of weight loss on the aluminide coated 304 sample. Furthermore, the coating layer is dense (D2 and E2) and Al inward diffusion has occurred during SCW exposure, reaching a depth of 55 μm (E2). The XRD analysis result, shown in Figure 9, confirms the presence of Al_2O_3 on the surface, in addition to an Al-rich $\alpha\text{-FeNi}$ in the coating layer.

3.2.3 Cr-modified Aluminide coating on 304

Cr-modified aluminide coated 304 sample experienced more weight loss than the aluminide coated samples, although the coating had a higher Al and Cr for protective oxide formation. Upon examining the exposed surface, it became clear that the spallation of oxide layer occurred. As shown in Figure 10, there are three distinct areas on the surface, A3 with Cr, Al and O, B3 covered with Fe enriched oxide and C3 which was exposed due to the spallation of B3 (“river pattern” can be seen on the exposed surface C3). Area B3 is characterized by a large concentration of Fe and some O and Al; the high concentration of Fe indicates either thin oxide (Fe from the metal substrate) or Fe-containing oxide formation (e.g. spinel) although this oxide could not be detected by XRD. Based on the SEM image (Figure 10), it is believed that B3 previously covered the area labelled C3. The spallation of Fe-containing oxide (B3) left the exposed area C3 at a lower elevation (ridges left from spallation of B3 are labeled with arrows in Figure 10). The composition measured from C3 indicates alumina formation below the Fe-containing oxide layer.

The cross section of the Cr-modified aluminide coated sample is present in Figure 11. The surface is covered with a layer of oxide (D3, ~10-15 μm), composed primarily of Al and Fe oxide. Beyond the non-uniform surface oxide, there is an evidence of internal oxidation in region E3 (grey particles), however, EDS was not able to detect oxygen due to the limited number and size of these individual particles. EDS results from regions D3 and E3 found a lower than usual Cr content since the sample was chromized to a high Cr content (28% after surface polishing prior to SCW exposure). Cr depletion must have occurred during SCW exposure, possibly through both oxide scale spallation and volatilization of chromium oxide formed on the surface [28], also contributing to a weight loss. Further below the internally oxidized region E3 is a region with single grey phase

(F3), likely being an Al-rich Fe(Ni) layer. In fact, XRD analysis (Figure 12) revealed the presence of both alumina and α -NiFe(Al) in the surface layer, confirming the SEM observation.

4.0 Discussion

Application of coating has the ability to improve environmental resistance while maintaining the structural integrity for various applications. For the current SCWR application, the fuel cladding must be able to withstand high temperatures, stress, and radiation, which leads to limitations on the use of some alloying elements, such as Co and excessive Ni. Covering Fe based alloys with coatings has the potential to improve alloy's oxidation/corrosion resistance, particularly for high temperature and high pressure corrosive SCW.

Upon exposure to oxidizing environment, metals will react with oxygen to form oxide. There are three key factors that characterize an oxidation process: the driving force, the nature/stability of the oxide film that forms (i.e., P-B ratio) and the rate at which oxidation occurs. The driving force is represented by the standard energy of formation for the oxide, also known as an Ellingham Diagram [32]. Al, in particular, has greater driving force for oxidation than most of other engineering metals such Fe, Ni, and Cr. In addition, the alumina formation has a near to 1 P-B ratio as such the oxide adhered to metal surface tightly [32]. Lastly, the rate of oxidation for Al (and Cr) exhibits a logarithm relationship with time, rendering a protective nature of the oxide once it covers the metal surface. For these reasons, many high temperature oxidation and corrosion coatings are primarily based on Al-containing alloys [33] [34]. Cr addition to alloys reduces the critical amount of Al required to form external alumina due to a gettering or third element effect [35] [36], allowing relatively ductile Al-containing coatings/alloys to be developed. Although the

addition of Cr alone has been observed to impart oxidation and corrosion resistance, chromium oxides are susceptible to steam induced volatility [27] [28]. Alumina forming coatings with Cr addition are therefore potentially more advantageous for high temperature SCW environment. Results from NiCrAlY and FeCrAlY coatings tested in SCW have shown promising results [37] [38]. Excellent steam oxidation resistance of iron aluminide coating on ferritic steel has also been observed at 650°C [39].

In this study, a pack aluminide and Cr-modified aluminide process was applied to 304 stainless steel. The pack process was selected for this study due to its versatility for large components and ability to reach non-line-of-sight locations. It has been employed in coating of low-Cr steels, such as P92 for steam power plant application [40]. Previous studies have shown that polishing surfaces to a 600 grit finish resulted in minimum weight change [41]. As such, coating developed must have sufficient thickness to allow for subsequent surface polishing while maintaining sufficient Al and/or Cr content. A coating process providing thicker alumina coating (~40 µm) was selected.

Based on the results from this study, bare 304 and two coated 304 samples experienced weight loss after 1000 h in SCW at 700°C and 25 MPa. Scale spallation was observed on bare 304 and Cr-modified aluminide coated 304 while the aluminide coated sample showed very small weight loss among the three. It also exhibited less weight loss than that observed on 800H tested in the same test batch (Figure 3). Weight loss resulted from oxide scale spallation is of a great concern in SCWR and steam turbines. The spalled scale can be circulated into the downstream, blocking and eroding components [42]. Application of aluminide coating is found in this study to have the potential to reduce the weight loss and hence scale spallation when being applied to 304 stainless steel.

Although aluminide coated 304 showed some weight loss in this study, results from steam test at the same temperature or SCW environment at lower temperature have yielded weight gains instead. For example, aluminide coating on P92 had a weight gain of about 1.5 mg/cm^2 after 1000 h in SCW at 650°C [43]. The application of an aluminide coating (about 60 at.%) on 304 resulted a weight gain of 0.15 mg/cm^2 [24] in 100% steam (not pressurized) at 700°C . In addition to the differences in the pressure, temperature and surface preparation procedures, the aluminide coating surface compositions and composition profiles vary greatly, affecting long term performance of coated alloys.

Cr has been observed to have the function of “a getter” or “third element effect” [36]. By adding Cr to an aluminide coating, it can alleviate the potential for cracking or spallation of pure alumina, as water/steam tends to lower the toughness of the alumina/substrate interface [44]. Furthermore, a Cr layer between Al and substrate has been observed to act as diffusion barrier, preventing the outward diffusion of Fe to the coating surface [45]. As such, Cr-modified aluminide coating was also selected in this study.

Cr-modified aluminide tested in steam at 650°C has previously showed weight gains after 1000 h [23]. Within the scope of this study, chromizing prior to aluminizing produced a coating with a higher weight loss. The reasons can be threefold. First, oxide scale formation is usually greater in SCW than that under steam condition with lower pressure [25]. The thicker scale, once spalled, would result in greater weight loss. Secondly, volatilization of chromium oxide [28] formed on the surface also could have contributed to weight loss on the Cr-modified aluminide coating. Thirdly, the elevated Al content in Cr-modified aluminide coating could have led to the spallation/cracking of outer oxide layer. In fact an increased Al content in an aluminide coating has been seen to cause scale cracking/spallation in our previous study [46]. Cracking of the oxide layer has shown to

further increase oxidation [47]. Indeed, the remaining oxide layer is much thicker on the Cr-modified aluminide coating than that on the aluminide coated ones, in addition to the occurrence of internal oxidation (Figure 11). In other studies Cr-modified aluminide coating was found to have about six times more weight gain than the pure aluminide coating when being tested in SCW at 650°C and 30 MPa [45], consistent with the thicker oxide on Cr-modified aluminide coated 304 observed in this study, although the spallation of thicker oxide resulted in weight loss. It seems that the addition of Cr in the coating, compounded by the higher Al content on the surface (after polishing process), promoted thicker scale formation which is also more brittle (due to higher Al). Subsequent scale spallation, due to thermal stress during cooling from SCW testing, yielded the weight loss observed. As austenitic stainless steels usually contain sufficient Cr, the native Cr is able to play the role of promoting alumina formation; as such Cr addition in the coating process may not be warranted.

Lastly, it is to be noted that the pack cementation process produces coatings with defects present on the surface as such post-coating polishing/surface finishing is required for SCWR application. This however will result in final coating compositions dependent upon the amount of surface removal, creating composition variations. It may potentially limit the application of this process.

Conclusion

In this study, bare and coated 304 stainless steel were evaluated after exposure to SCW at 700°C for 1000 h. The results showed that all three samples experienced weight loss. However, the aluminide coated 304 had the lowest rate of weight loss (-1.5×10^{-4} mg/cm² h). Although alumina was observed on both aluminide and Cr-modified aluminide, oxide spallation was observed on the

Cr-modified aluminide surface, contributing to a larger weight loss. Based on the results from this study, aluminide coating demonstrated superior performance than Cr-modified aluminide coating with compositions reported in this study. Bare stainless steel 304 is not suitable for extended service under SCW at 700°C, due to excessive oxidation and oxide scale spallation.

Acknowledgement:

Funding to the Canada Gen-IV National Program was provided by Natural Resources Canada through the Office of Energy Research and Development, Atomic Energy of Canada Limited, and Natural Sciences and Engineering Research Council of Canada. The funding of Academy of Finland project IDEA (Interactive modelling of fuel cladding degradation mechanisms) is gratefully acknowledged.

References

- [1] "World population to 2300," United Nations Department of Economic and Social, New York, 2004.
- [2] U. DOE, "Nuclear Energy Research Advisory Committee and Gen IV International Forum," 2002.
- [3] T. Schulenberg, H. Matsui, L. Leung and A. Sedov, "Supercritical water cooled reactors," in *GIF Symposium Proceedings and 2012 Annual Report*, San Diego, 2012.
- [4] M. Yetisir, M. Gaudet and D. Rhodes, "Development and integration of Canadian SCWR concept with counter-flow fuel assembly," in *ISSCWR-6*, Shenzhen, 2013.
- [5] R. Klueh, "Elevated temperature ferritic and martensitic steels and their application to future nuclear reactors," *Int Mat Rev*, vol. 50, pp. 287-310, 2005.
- [6] L. Zhang, F. Zhu, Y. Bao and R. Tang, "Corrosion tests of candidate fuel cladding and reactor internal structural materials," in *2nd Canada-China joint workshop on 'Supercritical water-cooled reactors'*, Toronto, 2010.
- [7] T. Allen, Y. Chen, X. Ren, K. Sridhara, L. Tan, G. Was, E. West and D. Guzonas, "Material performances in supercritical water," in *Comprehensive nuclear materials*, Amsterdam, Elsevier, 2012, pp. 279-326.
- [8] L. Greenwood, "A new calculation of thermal neutron damage and helium production in nickel," *J Nucl Mat*, vol. 115, pp. 137-142, 1983.
- [9] G. Was, P. Ampornrat, G. Gupta, S. Teyseyre, E. West, T. Allen, K. Sridharan, L. Tan, Y. Chen, X. Ren and C. Pister, "Corrosion and stress corrosion cracking in supercritical water," *J Nucl Mater*, vol. 371, pp. 176-201, 2007.
- [10] K. Murty and I. Charit, "Structural materials for Gen-IV nuclear reactor: challenges and opportunities," *J Nucl Mater*, vol. 383, pp. 189-195, 2008.
- [11] Y. Nakazono, T. Iwai and H. Abe, "General corrosion properties of modified PNC1520 austenitic stainless steel in supercritical water as fuel cladding candidate material for supercritical water reactor," *J Phy Conf Ser*, vol. 215, p. 012094, 2010.
- [12] R. Peraldi and B. Pint, "Effect of Ni and Cr contents on the oxidation behaviour of ferritic and austenitic model alloys in air with water vapor," *Oxidation of Metals*, vol. 61, pp. 463-483, 2004.
- [13] J. Bischoff, A. Motta, C. Eichfeld, R. Comstock, G. Cao and T. Allen, "Corrosion of Ferritic Martensitic Steels in Steam and Supercritical Water," *Journal of Nuclear Materials*, vol. 441, no. 1-3, pp. 604-611, 2013.

- [14] W. Callister, *Materials science and engineering an introduction*, New York: John Wiley & Sons Inc., 2007.
- [15] A. Fry, S. Osgerby and M. Wright, "Oxidation of alloys in steam environments- a review," *National Physical Laboratory Report MATC*, vol. 90, pp. 1-39, 2002.
- [16] S. Bsat and X. Huang, "Corrosion behaviour of alloy 800H in low density superheated steam," *ISIJ Int*, vol. 56, pp. 1067-1075, 2016.
- [17] P. Kritzer, "Corrosion in High-Temperature and Supercritical Water and Aqueous Solutions: A Review," *Journal of Supercritical Fluids*, vol. 39, pp. 1-29, 2004.
- [18] W. T. Tsai and K. E. Huang, "Microstructural Aspect and Oxidation Resistance of An Aluminide Coating on 310 Stainless Steel," *Thin Solid Film*, vol. 366, pp. 164-168, 2000.
- [19] S. C. Tjong, "Transmission Electron Microscopy Investigation of the Transient Oxides Formed on the Aluminide Coating on Inconel 625 Superalloy," *Surface and Coating Technology*, vol. 30, pp. 207-214, 1987.
- [20] F. J. Peres and S. Castaneda, "TG-Mass Spectrometry Studies in Coating Design for Supercritical Steam Turbine," *Materials and Corrosion*, vol. 59, no. 5, pp. 409-413, 2008.
- [21] D. K. Das, V. Singh and S. V. Joshi, "Evolution of Aluminide Coating Microstructure on Nickel-Base Cast Superalloy CM-247 in A Single-Step High-Activity Aluminizing Process," *Metallurgical and Materials Transactions*, vol. 29A, pp. 2173-2188, 1998.
- [22] A. Shaaban, S. Hayashi and K. Azumi, "Effects of Nano Metal Coatings on Growth Kinetics of α -Al₂O₃ Formed on Ni-50Al Alloy," *Oxidation of Metals*, vol. 82, pp. 85-97, 2014.
- [23] A. Aguero, I. Baraibar, V. M. R. Gonzalez and D. Plana, "Corrosion Resistance of Novel Coatings on Ferritic Steels for Oxycombustion-Supercritical Steam Boilers: Preliminary Results," *Oxidation of Metals*, vol. 85, pp. 263-281, 2016.
- [24] J. Marulanda-Arevalo and F. Perez-Trujillo, "Behavior of Aluminum Coating by CVD-FBR in Steam Oxidation at 700C," *Journal of Ciencia, Tecnologia y Futuro*, vol. 5, no. 4, pp. 75-84, 2014.
- [25] R. Sanchez, X. Huang and D. Guzonas, "Effect Of Water Density/Pressure On The Corrosion Behaviour of IN 625 And A286," *AECL Journal of Nuclear Reviews*, vol. 5, no. 2, pp. 333-343, 2016.
- [26] A. Galeriea, F. Toscana, M. M. J. Dupeuxa and G. Lucazeauc, "Stress and Adhesion of Chromia-Rich Scales on Ferritic Stainless Steels in Relation with Spallation," *Materials Research*, vol. 7, no. 1, pp. 81-88, 2004.
- [27] E. J. Opila, "Volatility of Common Protective Oxides in High-Temperature Water Vapor: Current Understanding and Unanswered Questions", *Materials Science Forum*, vol. 765, pp. 461-464, 2004.

- [28] J. Ehlers, D. E. S. E. Young, A. Tyagi, H. Penkalla, L. Singheiser and W. Quadackers, "Enhanced Oxidation of the 9% Cr Steel P91 in Water Vapour Containing Environments," *Corrosion Science*, vol. 48, no. 11, pp. 3428-3454, 2006.
- [29] C. N. Laboratories, "Evaluation of Fuel Cladding Materials for the Canadian SCWR Concept - Generation-IV Reactor Concepts," Internal Report No. 217-127000-ASD-001, 2014.
- [30] M. S. Elbakhshwan, S. K. Gill, A. K. Rumaiz, J. Bai, S. Ghose, R. B. Rebak and L. E. Ecker, "High-temperature Oxidation of Advanced FeCrNi Alloy in Steam Environment," *Applied Surface Science*, vol. 426, pp. 562-571, 2017.
- [31] S. Bsat, B. Xiao, X. Huang and S. Pentilla, "Oxidation behaviour of alloys 800H, 304 and 3033 in high temperature supercritical water," *Oxidation of Metals*, p. in press, 2017.
- [32] D. R. Askeland and W. J. Wright, *Science and Engineering of Materials*, Thomson-Engineering, 2015.
- [33] Lindblad, "A Review of the Behavior of Aluminide-Coated Superalloys," *Oxidation of Metals*, vol. 1, no. 1, pp. 143-170, 1969.
- [34] D. J. Young, *High Temperature Oxidation and Corrosion of Metals*, Elsevier, 2008.
- [35] A. S. Khanna, *Introduction to High Temperature Oxidation and Corrosion*, AMS International, 2002.
- [36] F. H. Stott, G. C. Wood and J. Stringer, "The influence of alloying elements on the development and maintenance of protective scales," *Oxidation of Metals*, vol. 44, pp. 113-145, 1995.
- [37] X. Huang, J. Li and D. Guzonas, "Characterization of FeCrAlY Alloy in Supercritical Water," *Corrosion Engineering Science and Technology*, vol. 50, no. 2, pp. 137-148, 2015.
- [38] X. Huang, "Developing Corrosion Prevention Coating Solution for Canadian SCWR Concept," *JOM*, pp. 480-488, 2016.
- [39] A. Aguero, R. Muelas, M. Gutierrez, R. Van Vulpen, S. Osgerby and J. P. Banks, "Cyclic Oxidation and Mechanical Behaviour of Slurry Aluminide Coatings For Steam Turbine Components," *Surface and Coating Technology*, vol. 201, pp. 6253-6260, 2007.
- [40] A. Aguero, V. Gonzalez, M. Gutierrez and R. Muelas, "Oxidation under Pure Steam: Cr-based Protective Oxides and Coatings," *Surface and Coating Technology*, vol. 237, pp. 30-38, 2013.
- [41] Y. F. Qian, "Corrosion Resistant Coating Materials for SCWR Application," Masters Thesis, Carleton University, 2012.
- [42] W. J. Quadackers, P. J. ennis, J. Zurek and M. Michalik, "Steam Oxidation of Ferritic Steels—laboratory Test Kinetic Data," *Materials at High Temperatures*, vol. 22, pp. 47-60, 2005.

- [43] M. Scheefer, M. B. Henderson, A. Agüero, B. Allcock, B. Norton, D. N. Tsipa and R. Durham, "Development and Validation of Advanced Oxidation Protective Coatings for Super Critical Steam Power Generation Plants," in *Conference: Materials for Advanced Power Engineering, At Liege, Belgium, Volume: III*, 2006.
- [44] M. C. Maris-Sida, G. H. Meier and F. S. Pettit, "Some Water Vapour Effects During the Oxidation of Alloys that are alpha-Al₂O₃ Formers," *Metallurgical and Materials Transactions A*, vol. 34A, pp. 2609-2619, 2003.
- [45] Z. D. Xiang, S. R. Rose, P. K. Datta and M. Scheeffer, "Steam Oxidation Resistance and Thermal stability of Chromium Aluminide/Chromium Hybrid Coating on Alloy Steels Formed at Low Temperatures," *Surface and Coating Technology*, vol. 203, pp. 1225-1230, 2009.
- [46] T. Tabikh, M. El-Makdah, X. Huang and D. Guzonas, "Corrosion Performance of Aluminized IN 625 and Hastelloy-X in Supercritical Water Condition at 500°C," in *43. T. Tabikh, M. El-Makdah, Xiao Huang and D. Guzonas, CorroThe 3rd China-Canada Joint Workshop on Supercritical Water-Cooled Reactors (CCSC-2012)*, ChongQing, China, April, 2012.
- [47] B. A. Pint, Y. Zhang, L. R. Walker and I. G. Wright, "Long-term Performance of Aluminide Coatings on Fe-based Alloys," *Surface and Coatings Technology*, vol. 202, pp. 637-642, 2007.

Accepted Manuscript Not Copyedited

List of Tables

Table No.	Caption
Table 1	Composition of 304, 800H and 3033 (wt.%)
Table 2	Surface chemical compositions of aluminide and Cr-modified aluminide CVD coatings after polishing (wt.%)
Table 3	Sample initial weights (g) and dimensions (mm)

Table 1: Composition of 304, 800H and 3033 (wt.%)

Alloy	Fe	Ni	Cr	Mn	C	Si	S	Al	P	Ti	N	Mo	Cu
304	Bal.	10	19	2	0.08	0.75	0.03	--	0.05	--	0.10	--	--
800H*	Bal.	32.5	21	1.5	0.08	1.0	0.02	0.38	0.045	0.38	--	--	--
3033*	Bal.	31.5	33	1	0.08	0.25	--	--	0.01	--	0.48	1.25	0.75

*compositions of these alloys added for comparison purpose.

Table 2: Surface chemical compositions of aluminide and Cr-modified aluminide CVD coatings after polishing (wt.%)

Elements	Aluminide	Cr-modified aluminide
Al	10.9	16.9
Cr	19.7	29.4
Ni	7.2	9.3
Mn	1.3	0.7
Fe	60.4	43.7
Si	0.5	-

Table 3: Sample initial weights (g) and dimensions (mm)

	Weight prior to testing (g) (± 0.001 g)	Dimensions $l \times w \times t$ (mm) (± 0.02 mm)	Weight after SCW testing (g) (± 0.001 g)
Aluminide	4.745	21.76×20.41×1.46	4.743
Cr-Modified aluminide	4.803	21.76×20.74×1.48	4.773
Bare 304	2.649	19.72×12.53×1.49	2.608

List of Figures

Figure No.	Caption
Figure 1	(a) Aluminide and (b) Cr modified aluminide coatings (depth indicated by the arrows) in the as-coated condition (before surface polishing).
Figure 2	A schematic representation of the SCW autoclave system with water recirculation loops. The system consists of low and high pressure water recirculation loops in addition to the materials testing autoclave.
Figure 3	Weight change after 1000 h of exposure to SCW at 700°C.
Figure 4	Surface microstructure of bare 304 after 1000 h of exposure in SCW at 700°C.
Figure 5	Cross section of bare 304 after 1000 h of exposure in SCW at 700°C.
Figure 6	XRD spectrum of bare 304 after 1000 h of exposure in SCW at 700°C.
Figure 7	Surface microstructure of aluminide coated 304 after 1000 h of exposure in SCW at 700°C.
Figure 8	Cross section of aluminide coated 304 after 1000 h of exposure in SCW at 700°C.
Figure 9	XRD spectrum of aluminide coated 304 after 1000 h of exposure in SCW at 700°C.
Figure 10	Surface microstructure of Cr-modified aluminide coated 304 after 1000 h of exposure in SCW at 700°C.
Figure 11	Cross section of Cr-modified aluminide coated 304 after 1000 h of exposure in SCW at 700°C.
Figure 12	XRD spectrum of Cr-modified aluminide coated 304 after 1000 h of exposure in SCW at 700°C.

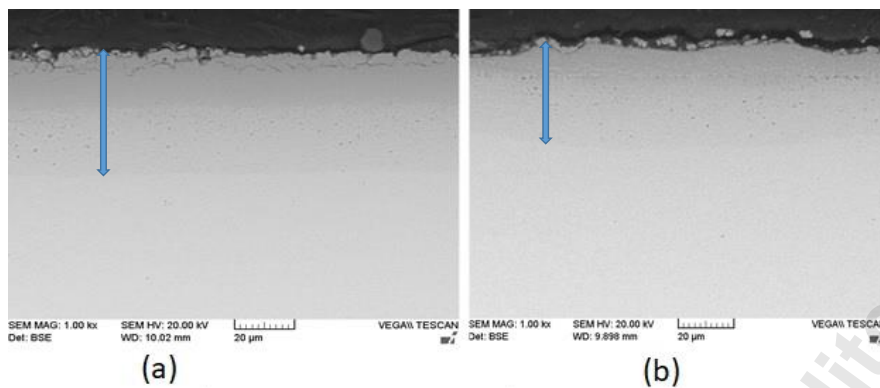


Figure 1: (a) Aluminide and (b) Cr modified aluminide coatings (depth indicated by the arrows) in the as-coated condition (before surface polishing).

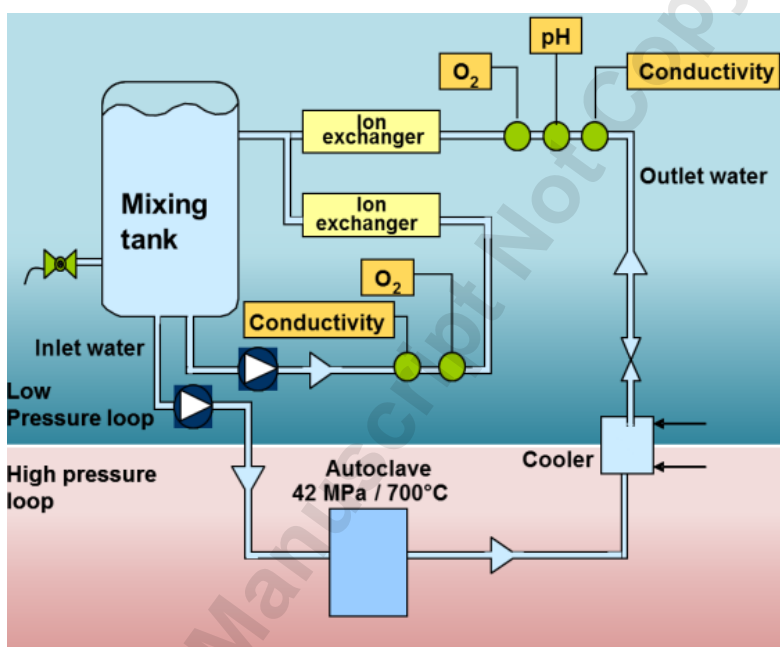


Figure 2: A schematic representation of the SCW autoclave system with water recirculation loops. The system consists of low and high pressure water recirculation loops in addition to the materials testing autoclave.

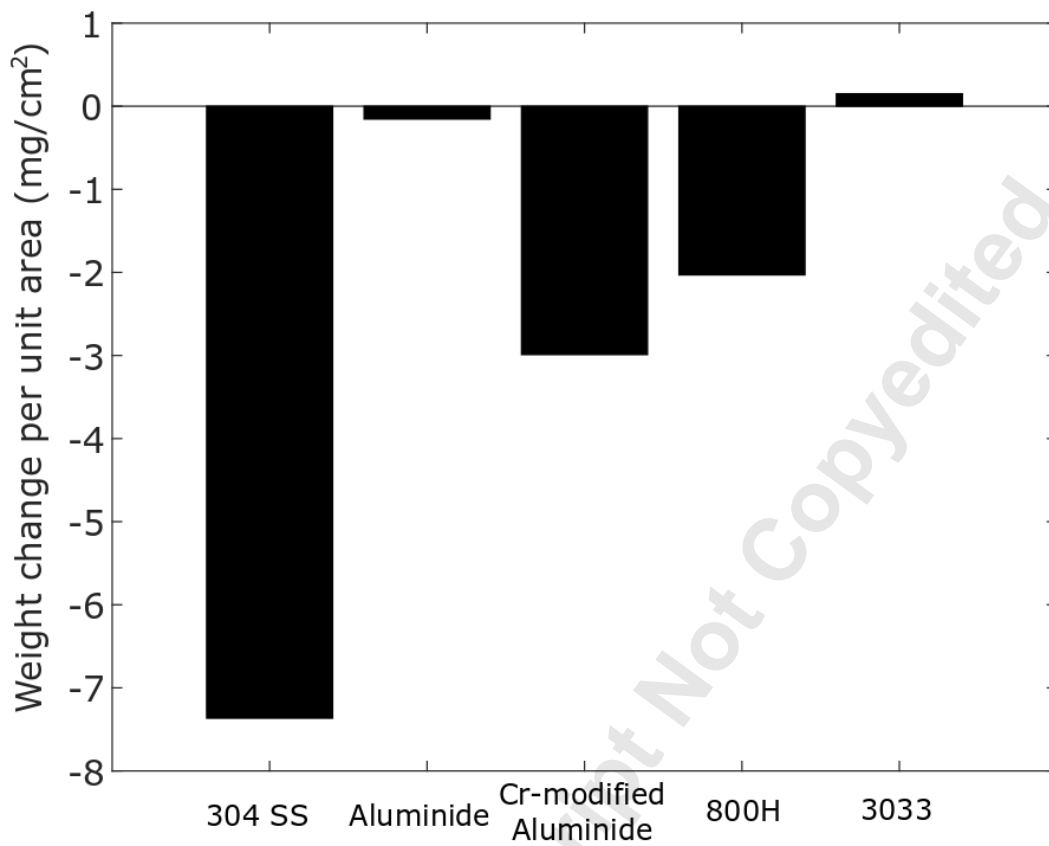


Figure 3: Weight change after 1000 h of exposure to SCW at 700°C.

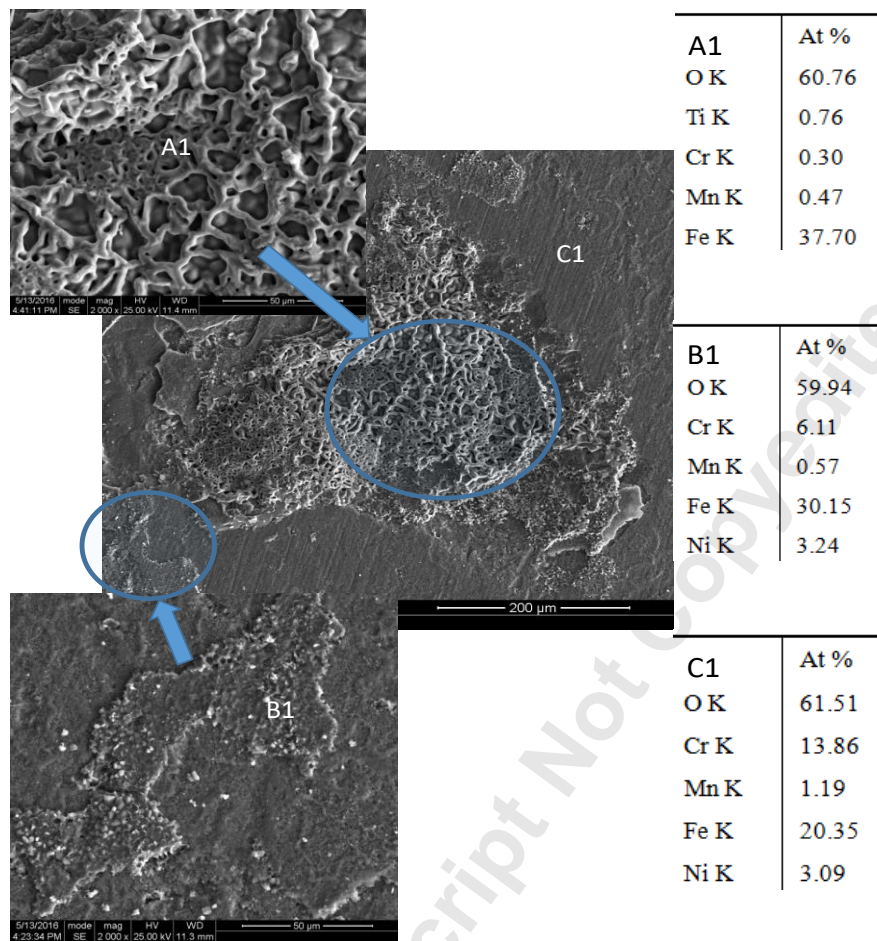


Figure 4: Surface microstructure of bare 304 after 1000 h of exposure in SCW at 700°C.

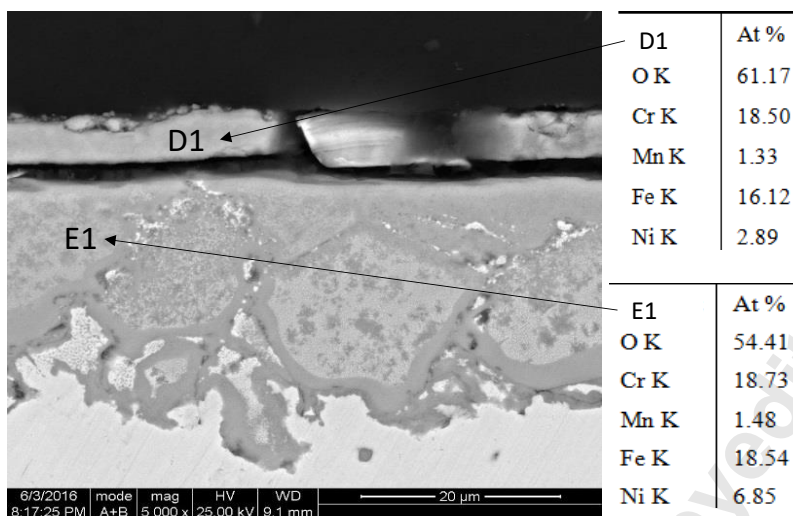


Figure 5: Cross section of bare 304 after 1000 h of exposure in SCW at 700°C.

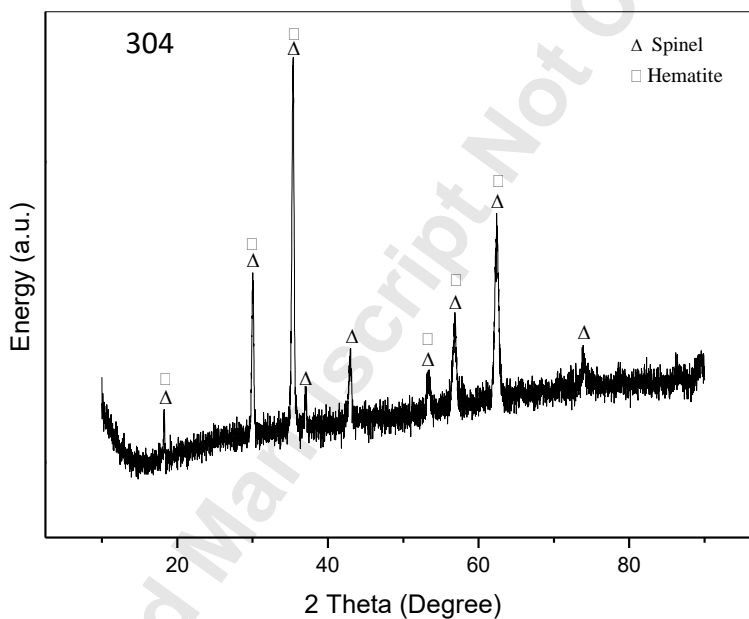


Figure 6: XRD spectrum of bare 304 after 1000 h of exposure in SCW at 700°C.

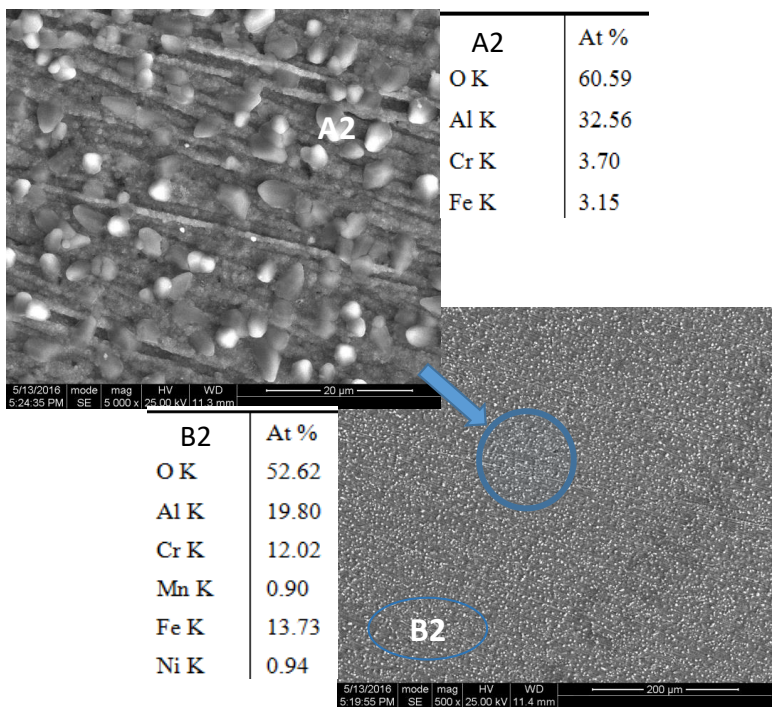


Figure 7: Surface microstructure of aluminide coated 304 after 1000 h of exposure in SCW at 700°C.

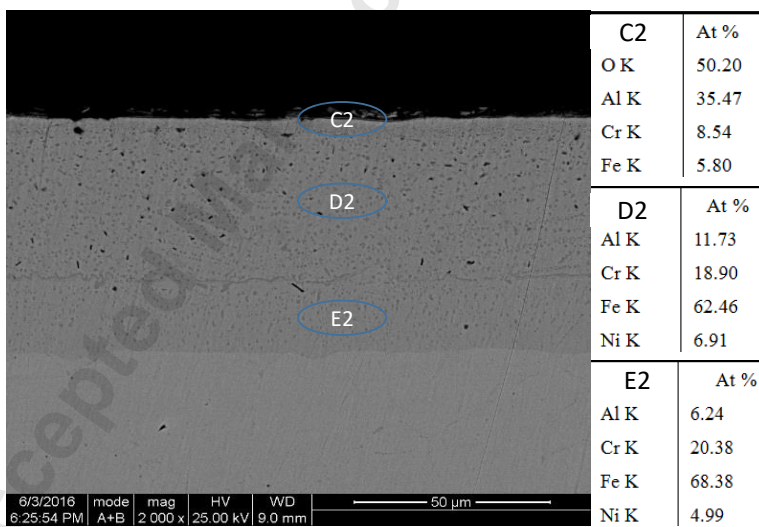


Figure 8: Cross section of aluminide coated 304 after 1000 h of exposure in SCW at 700°C.

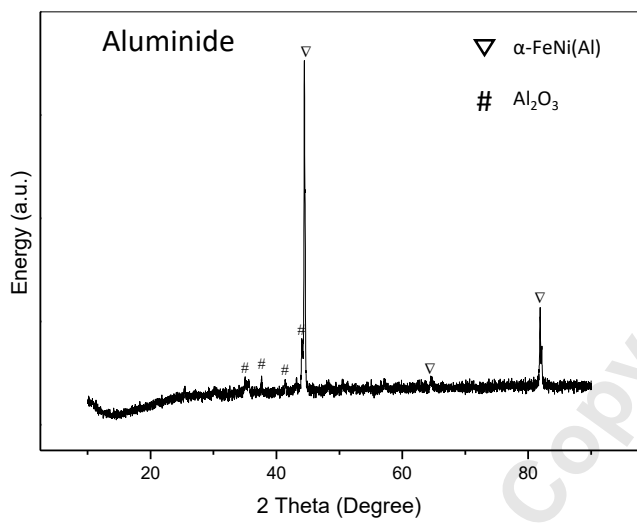


Figure 9: XRD spectrum of aluminide coated 304 after 1000 h of exposure in SCW at 700°C.

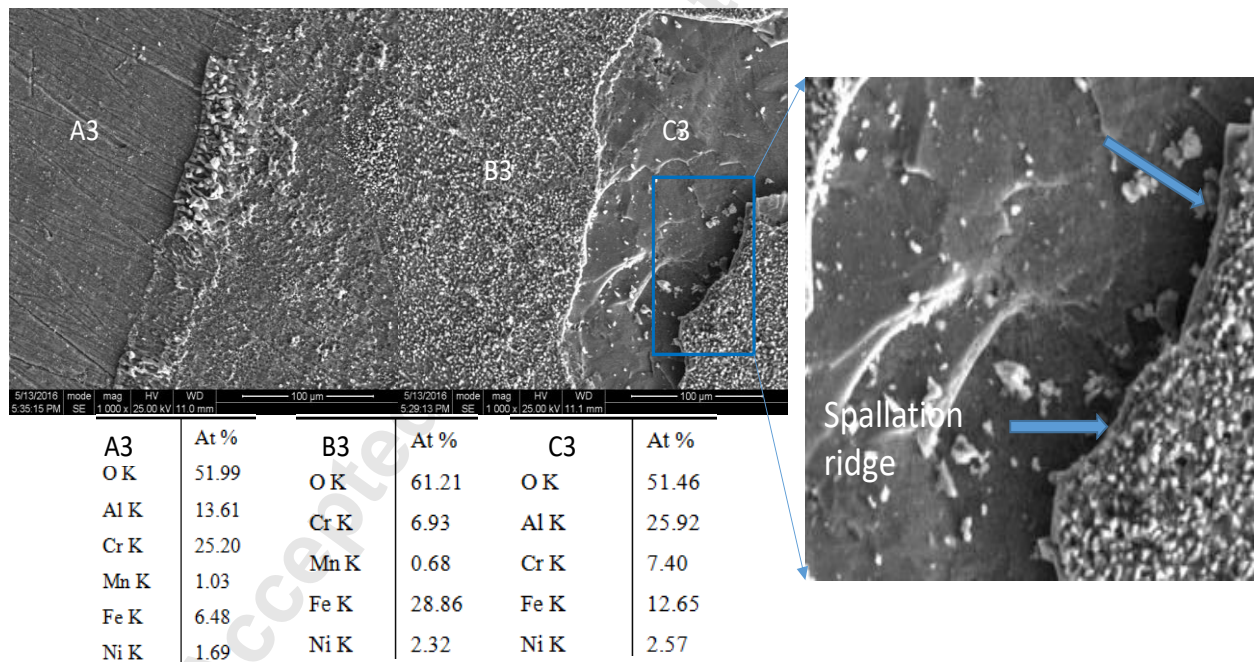


Figure 10: Surface microstructure of Cr-modified aluminide coated 304 after 1000 h of exposure in SCW at 700°C.

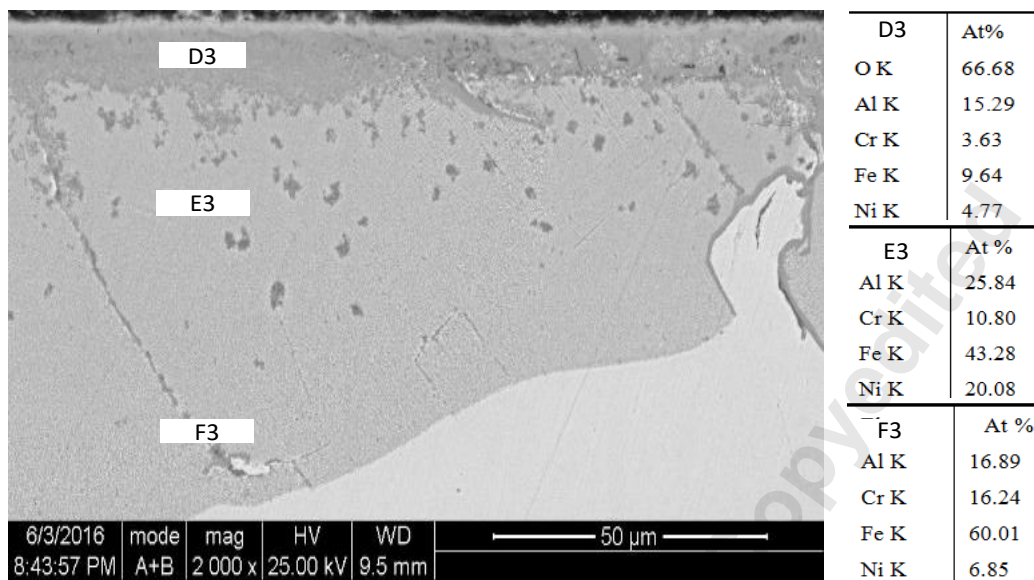


Figure 11: Cross section of Cr-modified aluminide coated 304 after 1000 h of exposure in SCW at 700°C.

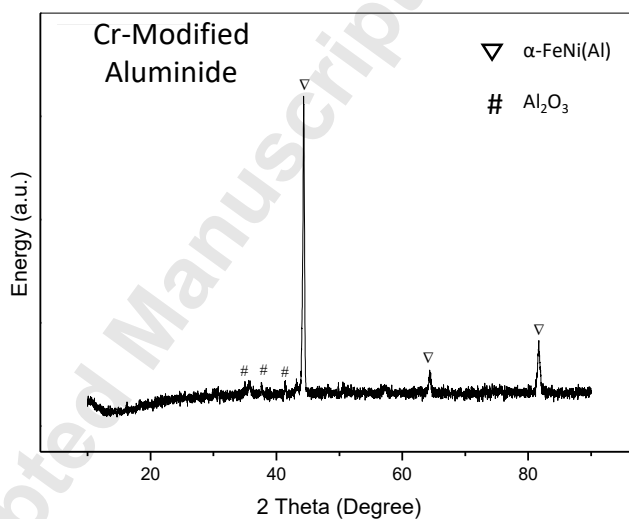


Figure 12: XRD spectrum of Cr-modified aluminide coated 304 after 1000 h of exposure in SCW at 700°C.